

Investigating Simple Drawings of K_n using SAT

Helena Bergold 

Manfred Scheucher 

Abstract

We present a SAT framework which allows to investigate properties of simple drawings of the complete graph K_n using the power of AI. In contrast to classic imperative programming, where a program is operated step by step, our framework models mathematical questions as Boolean formulas which are then solved using modern SAT solvers. Our framework for simple drawings is based on a characterization via rotation systems and finite forbidden substructures. We showcase its universality by addressing various open problems, reproving previous computational results and deriving several new computational results. In particular, we test and progress on several unavoidable configurations such as variants of Rafla’s conjecture on plane Hamiltonian cycles, Harborth’s conjecture on empty triangles, and crossing families for general simple drawings as well as for various subclasses. Moreover, based on our computational results we propose some new challenging conjectures.

2012 ACM Subject Classification Mathematics of computing → Discrete mathematics; Mathematics of computing → Geometric topology; Mathematics of computing → Solvers; Human-centered computing → Graph drawings; Hardware → Theorem proving and SAT solving; Theory of computation → Automated reasoning; Theory of computation → Computational geometry

Keywords and phrases Boolean satisfiability problem (SAT), automated reasoning, automated theorem proving, artificial intelligence, planar graph, simple drawing

Supplementary Material <https://github.com/manfredscheucher/rotsys-sat>

1 Introduction

In logic and computer science, the Boolean satisfiability problem (SAT) is the problem of determining whether a finite formula on Boolean variables has an assignment such that the formula evaluates to True. SAT is the first problem that was proven to be NP-complete, which asserts that there is no efficient algorithm for the SAT problem unless $P = NP$. Over the last years, however, the area of SAT solving has seen tremendous progress and many problems that seemed to be out of reach a decade ago can now be handled routinely [30, 12, 29, 21, 32].

In this article we present a versatile SAT framework for investigating simple drawings of the complete graph K_n . In contrast to arbitrary drawings of a fixed graph, which can be arbitrarily complex, *simple* drawings can be encoded by a finite Boolean formula. A drawing of a graph is *simple* if every pair of edges has at most one common point, which is either a crossing or a common endpoint.

Many properties that are in focus of active research such as plane Hamiltonian cycles or empty triangles do not depend on the actual drawing but only on the underlying combinatorics of the drawing. More specifically, the purely combinatorial information about the pairs of crossing edges and the cyclic orders around the vertices – the so-called *rotation system* of the drawing – is sufficient to study many problems.

A crucial ingredient of our framework is a theorem by Kynčl [37] together with the computational result by Ábrego et al. [1]. It gives a compact characterization which systems of cyclic permutations are in fact a rotation system of a simple drawing. We give the precise definitions and the characterization in Section 2. In Section 3 we describe the encoding of the combinatorial structures such that the solutions are in correspondence with rotation systems. Since the default input format of SAT solvers are Boolean formulas in conjunctive normal form (CNF), we present a list of clauses which are then conjugated (logical “AND”) to one

formula. A clause is a disjunction (logical “OR”) of literals, where a literal is a Boolean variable or its negation. For more background see the standard textbook [18]. In Appendix A we moreover develop a SAT encoding for checking whether a system comes from a drawing and give an alternative proof of the characterization of Ábrego et al. [1].

Additionally to the general setting of simple drawings, our framework allows to restrict the search space to certain subclasses that appear in active research. Among them are convex, hereditary convex, c -monotone, strongly c -monotone or generalized twisted drawings. All of these subclasses can be characterized in terms of the rotation system and yield a reasonably compact SAT encoding; see Section 4 for more details.

In Section 5, we showcase the power of our framework. We formulate various open problems related to simple drawings of the complete graph as a CNF and test several conjectures for small values. In particular, we focus on the existence of plane Hamiltonian cycles and other plane substructures related to Rafla’s conjecture (Sections 5.1 and 5.2), the existence of uncrossed edges and crossing families (Sections 5.3 and 5.4), unavoidable subdrawings of the complete graph (Section 5.5), and the number of empty triangles (Section 5.6).

The previously best computational results were obtained using enumerative and brute-force approaches [1]. However, as there exist approximately 7 billion rotation systems of K_9 and the number of rotation systems of K_n grows as $2^{\Theta(n^4)}$ [36], an enumerative approach for $n = 10$ will not be possible in reasonable time with contemporary computers. Our novel SAT-based framework certainly surpasses these previous approaches as it allows to make investigations for 10 to 15 vertices with reasonably small resources – of course depending on the desired property. Moreover, our framework gives an excellent computational basis for searching for drawings on 20 or more vertices with certain properties (cf. Section 5.5), even though a complete search seems unlikely at the current stage.

2 Preliminaries

Various properties of a simple drawing only depend on the combinatorics of the drawing. For example, to determine the existence of plane substructures, it is sufficient to know which pairs of edges cross – the actual routing of edges does not play a role. More generally, we will make extensive use of the cyclic orders of edges around the vertices, which in particular capture the information about crossing edge pairs. In this article we only consider properties which do not depend on the choice of the unbounded cell. Hence, in the following we often do not distinguish between drawings on the sphere and drawings in the plane.

For a given simple drawing \mathcal{D} and a vertex v of \mathcal{D} , the cyclic order π_v of incident edges in counterclockwise order around v is called the *rotation of v* in \mathcal{D} . The collection of rotations of all vertices is called the *rotation system* of \mathcal{D} . In the case of the complete graph $K_n = (V, E)$, the rotation of a vertex v is a cyclic permutation on the remaining $n - 1$ vertices $V \setminus \{v\}$.

A *pre-rotation system* on V consists of cyclic permutations π_v on the elements $V \setminus \{v\}$ for all $v \in V$. A pre-rotation system $\Pi = (\pi_v)_{v \in V}$ is *drawable* if there is a simple drawing of the complete graph with vertices V such that its rotation system coincides with Π . Two pre-rotation systems are *isomorphic* if they are the same up to relabelling and reflection (i.e., all cyclic orders are reversed). Two simple drawings are *weakly isomorphic* if their rotation systems are isomorphic. Note that there exist several types of isomorphisms in literature.

On four vertices there are three non-isomorphic pre-rotation systems. The K_4 has exactly two non-isomorphic simple drawings on the sphere: the drawing with no crossing and the drawing with one crossing; see Figure 1. Hence, the two corresponding pre-rotation systems

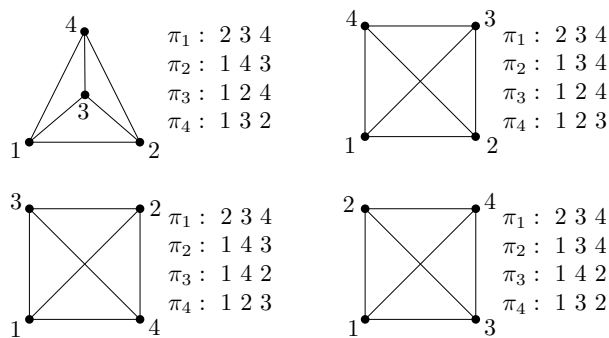


Figure 1 The four rotation systems on 4 elements with their drawings. The second, third, and fourth are isomorphic. The first one represents the second isomorphism class.

are drawable, and the third pre-rotation system is an obstruction to drawability. It is denoted by Π_4^o and described in Figure 2.

Π_4^o : π_1 : 2 3 4 π_2 : 1 3 4 π_3 : 1 2 4 π_4 : 1 3 2	$\Pi_{5,1}^o$: π_1 : 2 3 4 5 π_2 : 1 3 4 5 π_3 : 1 4 2 5 π_4 : 1 5 3 2 π_5 : 1 4 2 3	$\Pi_{5,2}^o$: π_1 : 2 3 4 5 π_2 : 1 3 5 4 π_3 : 1 4 2 5 π_4 : 1 5 3 2 π_5 : 1 2 4 3
---	--	--

Figure 2 The three obstructions Π_4^o , $\Pi_{5,1}^o$, and $\Pi_{5,2}^o$ for rotation systems.

For a pre-rotation system $\Pi = (\pi_v)_{v \in V}$ and a subset of the elements $I \subseteq V$, the *sub-configuration induced by I* is $\Pi|_I = (\pi_v|_I)_{v \in I}$, where $\pi_v|_I$ denotes the cyclic permutation obtained by restricting π_v to $I \setminus \{v\}$. A pre-rotation system Π on V *contains* Π' if there is an induced subconfiguration $\Pi|_I$ with $I \subseteq V$ isomorphic to Π' . A pre-rotation system not containing Π' is called Π' -free.

A crossing pair of edges involves four vertices. By studying drawings of K_4 we learn that a crossing pair of edges can be identified from the underlying rotation system. Hence, the pairs of crossing edges in a drawing of K_n are fully determined by the rotation system.

► **Lemma 2.1.** *The following two statements hold:*

- (i) *A pre-rotation system containing Π_4^o is not drawable.*
- (ii) *Let Π be a Π_4^o -free pre-rotation system on $[n]$. The subconfiguration induced by a 4-element subset is drawable and determines which pairs of edges cross in the drawing.*

Part (ii) of the lemma allows to talk about the crossing pairs of edges of a Π_4^o -free pre-rotation system, even if there is no associated drawing. Ábrego et al. [1] generated all pre-rotation systems for up to 9 vertices and used a drawing program based on back-tracking to classify the drawable ones.

► **Proposition 2.2** ([1]). *A pre-rotation system on $n \leq 6$ elements is drawable if and only if it does not contain Π_4^o , $\Pi_{5,1}^o$, or $\Pi_{5,2}^o$ (cf. Figure 2) as a subconfiguration.*

Moreover, Kynčl showed that a pre-rotation system is drawable if and only if all induced 4-, 5-, and 6-element subconfigurations are drawable [37, Theorem 1.1]. Together with Proposition 2.2 this yields the following characterization:

► **Theorem 2.3.** *A pre-rotation system on n elements is drawable if and only if it does not contain Π_4^o , $\Pi_{5,1}^o$ or $\Pi_{5,2}^o$ (cf. Figure 2) as a subconfiguration.*

While the focus of this article is on the structural investigation of simple drawing of K_n , we provide an independent proof of Proposition 2.2 in Appendix A, which utilizes SAT solvers on two levels. First we use a SAT solver to enumerate all non-isomorphic pre-rotation systems. Then, for each pre-rotation system, we create a SAT instance to test its drawability. More specifically, to decide whether a given pre-rotation system yields a drawing, we read the crossings along each edge (cf. Lemma 2.1) and then use SAT to find an ordering of the crossings along all edges so that the obtained subdivided graph corresponds to a planarization of a drawing. To ensure planarity, we utilize Schnyder’s characterization of planar graphs [45]; see Appendix B. For further details and more planarity encodings suitable for the SAT-based investigations of planar graphs we refer the interested reader to [35].

3 SAT Encoding

We develop a versatile SAT framework for rotation systems of simple drawings of K_n . It comes with many optional parameters that make it possible to search for examples with (a combination of) certain properties and to restrict the search to certain subclasses. To verify conjectures for small n one can then create a specific CNF instance to search for a counterexample and use a SAT solver such as CaDiCaL [17] to prove unsatisfiability. It is worth noting that unsatisfiability can also be certified with an independent proof-verification tool such as drat-trim [49]. In the following we describe the basic encodings.

3.1 Pre-Rotation Systems

A pre-rotation system on $[n]$ consists of n cyclic permutations π_a on $[n] \setminus \{a\}$. One way to encode the cyclic permutations in terms of a CNF is to use ordinary permutations. For this we introduce a Boolean variable X_{aib} for every pair of distinct vertices $a, b \in [n]$ and every index $i \in [n-1]$, to indicate whether $\pi_a(i) = b$. To ensure that for every $a \in [n]$ the variables X_{aib} indeed model a permutation π_a , we introduce clauses such that for every $i \in [n-1]$ there is exactly one $b \in [n] \setminus \{a\}$ for which X_{aib} is True. More formally, we use the clauses

- $\bigvee_{b:b \neq a} X_{aib}$ for every $a \in [n]$ and $i \in [n-1]$, and
- $\neg X_{aib_1} \vee \neg X_{aib_2}$ for every distinct $a, b_1, b_2 \in [n]$ and $i \in [n]$.

The first clause ensures that for fixed a and i at least one of the variables X_{aib} is True, and the second implies that at most one is True. Since we deal with cyclic permutations, we assume without loss of generality that the first element in a permutations is the smallest. Therefore, we add the unit clauses

- $X_{112} = \text{True}$ and $X_{k11} = \text{True}$ for $k \geq 2$.

Since the X -variables only give us a “global” description of the entire rotation system, we introduce additional auxiliary variables to describe the rotation system around each vertex in more detail. We introduce an auxiliary variable Y_{abcd} for every four distinct vertices $a, b, c, d \in [n]$ to indicate whether b, c, d appear in counterclockwise order in the rotation of a . Note that precisely one of two variables Y_{abcd} and Y_{abdc} is True, and that $Y_{abcd} = Y_{acdb} = Y_{adbc}$. To synchronize the X -variables with the Y -variables, we assert for every distinct $a, b, c, d \in [n]$ and $i, j, k \in [n-1]$ that

- $(X_{aib} \wedge X_{ajc} \wedge X_{akd}) \rightarrow Y_{abcd}$ if $i < j < k$ or $k < i < j$ or $j < k < i$, and
- $(X_{aib} \wedge X_{ajc} \wedge X_{akd}) \rightarrow \neg Y_{abcd}$ if $i < k < j$ or $k < j < i$ or $j < i < k$.

To model this as a CNF, we use that $(A_1 \wedge \dots \wedge A_k) \rightarrow B$ is logically equivalent to $\neg A_1 \vee \dots \vee \neg A_k \vee B$. While the above encoding derives the values of the Y -variables from the X -variables, we describe in the following how to directly encode the cyclic permutations only in terms of the Y -variables. In fact, when we used the SAT solver CaDiCaL we observed

that the following clauses were learned after some time. By adding these clauses to the CNF, the solver performed significantly faster.

A mapping $\sigma : \binom{X}{3} \rightarrow \{+, -\}$ encodes a *cyclic permutation* if for all distinct four elements i, j, k, ℓ with $i < j < k < \ell$ the sign sequence $(\sigma(i, j, k), \sigma(i, j, \ell), \sigma(i, k, \ell), \sigma(j, k, \ell))$ is one of the following six: $\{(+, +, +, +), (+, +, -, -), (+, -, -, +), (-, -, -, -), (-, -, +, +), (-, +, +, -)\}$. In other words the following ten sign patterns are forbidden:

$$\{(+, -, +, -), (-, +, -, +), (+, -, -, -), (-, +, -, -), (-, -, +, -), \\ (-, -, -, +), (-, +, +, +), (+, -, +, +), (+, +, -, +), (+, +, +, -)\}$$

To forbid the pattern $(+, -, +, -)$ for each $a \in [n]$ and all $b < c < d < e$ from $[n] \setminus \{a\}$, we use the following clause:

- $\neg Y_{abcd} \vee Y_{abce} \vee \neg Y_{abde} \vee Y_{acde}$

The other patterns are forbidden analogously. To further improve the encoding, these ten clauses of length 4 can be replaced by the following eight clauses of length 3:

- $\neg Y_{abcd} \vee Y_{abce} \vee \neg Y_{abde}$
- $Y_{abcd} \vee \neg Y_{abce} \vee Y_{abde}$
- $\neg Y_{abce} \vee Y_{abde} \vee \neg Y_{acde}$
- $Y_{abce} \vee \neg Y_{abde} \vee Y_{acde}$
- $\neg Y_{abcd} \vee \neg Y_{abde} \vee Y_{acde}$
- $Y_{abcd} \vee Y_{abde} \vee \neg Y_{acde}$
- $\neg Y_{abcd} \vee Y_{abce} \vee Y_{cbde}$
- $Y_{abcd} \vee \neg Y_{abce} \vee \neg Y_{cbde}$

3.2 Rotation System

To restrict the search space to drawable pre-rotation systems, that is, rotation systems of the complete graph K_n , we introduce clauses to forbid the drawability-obstructions. Theorem 2.3 asserts that a pre-rotation system is drawable if and only if none of the obstructions Π_4^o , $\Pi_{5,1}^o$ and $\Pi_{5,2}^{oc}$ (depicted in Figure 2) occur as a substructure. To ensure that the obstructions Π_4^o or its reversed does not occur in any induced subconfiguration, the two clauses

- $\neg Y_{abcd} \vee \neg Y_{bacd} \vee \neg Y_{cabd} \vee \neg Y_{dacb}$ and $Y_{abcd} \vee Y_{bacd} \vee Y_{cabd} \vee Y_{dacb}$

must be fulfilled for every four distinct vertices $a, b, c, d \in [n]$. In an analogous manner, we can forbid $\Pi_{5,1}^o$ and $\Pi_{5,2}^{oc}$ as subconfigurations. In total, we have $\Theta(n^5)$ clauses to assert that solutions of the CNF are in one-to-one correspondence with rotation systems on $[n]$ elements.

By enabling the flags `-v4` and `-v5` one can disable the above clauses for valid 4-tuples and valid 5-tuples, respectively, and enumerate pre-rotation systems.

3.3 Symmetry Breaking

Since most properties discussed in this article are invariant to relabeling and reflection, we attempt to break these symmetries to get a one-to-one correspondence between the solutions of the CNF and the isomorphism classes of (pre-)rotation systems.

Since there are $n!$ relabelings of the vertices and the possibility of reflection, there are up to $2n!$ (pre-)rotation systems in a weak isomorphism class. We define a unique representative of every isomorphism class. For this, observe that the X -variables of a pre-rotation system Π can be read as an $n \times (n-1)$ matrix, where the a -th row encodes the permutation of the a -th element. By concatenating the rows of the matrix, we consider a vector of length $n \cdot (n-1)$. The *lexicographic minimal* vector among all relabelings and reflections is our representative.

At first glance, it seems that we have to check all $n!$ relabellings and their reflections to determine whether a pre-rotation system Π is a lexicographic minimum. However, the lexicographic minimum has to be *natural*, that is, the rotation around the first vertex is the identity permutation. To assert that a pre-rotation system is natural, we use the unit clauses:

- $Y_{1abc} = \text{True}$ for all $a, b, c \in [n] \setminus \{1\}$ such that $a < b < c$.

Being natural is only a necessary condition but not sufficient; see for example the three natural rotation systems of K_4 with a crossing depicted in Figure 1. However, since the choice of the first and second vertex in a natural labeling fully determines the first row and thus the full permutation of the vertices, we only have to test $n(n-1)$ relabellings and their reflections. Recall that we do not actually run an algorithm to perform those tests but ingeniously add constraints to the CNF so that all solutions fulfill the desired properties.

Besides the identity permutation on $[n] \setminus \{1\}$ in the first row of the matrix in a natural pre-rotation system, we further assume that the first element in every row is the smallest one of the cyclic permutation. To ensure that it is a lexicographical minimum, we introduce auxiliary variables and clauses to compute the 0-1-vector of all $2n(n-1) - 1$ reflections and relabelings. Additional constraints in terms of the X -variables assert that the original vector is indeed the lexicographically smallest. Since the encoding in terms of Boolean variables is quite technical, we omit the details and refer the interested reader to the source code [16].

While our framework by default restricts the search space to natural rotation systems (this can be disabled via the flag `-nat`), the restriction to lexicographic minima needs to be explicitly enabled using the flag `-lex` as it seems to be quite expensive in practice. Even though it should reduce the search space by a factor of up to $2n(n-1)$ in theory, SAT solvers are slowed down in practice due to the large amount of auxiliary variables and clauses.

3.4 Crossings

Many open questions related to simple drawings concern plane substructures and crossings. To encode crossings in terms of a CNF we introduce auxiliary variables $C_{abcd} = C_{ef}$ to indicate whether two non-adjacent edges $e = \{a, b\}$ and $f = \{c, d\}$ cross (cf. Lemma 2.1(ii)). If the drawing of K_4 with vertices $\{a, b, c, d\}$ is crossing-free, the rotation system is unique up to relabelling or reflection. Otherwise, if there is a crossing, we have one of the following: ab crosses cd , ac crosses bd , or ad crosses bc and this is fully determined by the rotation system. For each of these three cases, there are two subcases. If ab crosses cd , then the directed edge \vec{cd} either traverses \vec{ab} from the left to the right or vice versa. Each subcase corresponds to a unique rotation system. The three cases are depicted in Figure 1. The other cases are the reversed rotation systems which correspond to the reflected drawings. To indicate the subcase, we introduce an auxiliary variables D_{abcd} and the clauses $C_{abcd} = D_{abcd} \vee D_{abdc}$.

To prove that every simple drawing of K_n has a particular structure, we encode the contraposition. Solutions of the CNF encode potential examples which violate this structure. If the CNF is unsatisfiable, the statement follows. For more details see Appendix C.1.

4 Subclasses

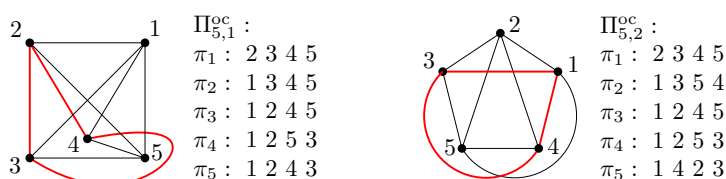
Our framework comes with plenty of optional parameters to restrict the search space and/or to require certain properties. In the following we discuss some subclasses that can be fully characterized in terms of the rotation system and moreover yield a reasonably sized encoding in terms of a CNF. For a detailed overview of subclasses studied in literature and their relationships we refer to [8, Figure 7].

4.1 Convex and H-convex Drawings

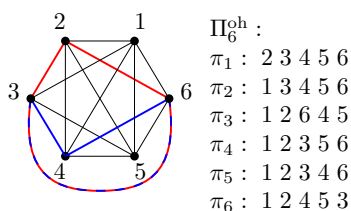
Convex drawings are a subclass between *geometric* drawings where all edges are drawn as straight-line segments and simple drawings. As indicated by the name, they generalize the

classical notion of convexity. To give a formal definition, we need to look at the *triangles*, i.e., the subdrawings induced by triples of vertices. Since in a simple drawing of K_n the edges of a triangle do not cross, a triangle partitions the plane (resp. sphere) into exactly two connected components. The closures of these components are the two *sides* of the triangle. A side S of a triangle is *convex* if every edge that has its two vertices in S is fully drawn inside S . A simple drawing of K_n is *convex* if every triangle has a convex side. Moreover, a drawing is *h-convex* (short for hereditary convex) if we can choose a convex side S_T for every triangle T such that, for every triangle T' contained in S_T , it holds $S_{T'} \subseteq S_T$. For further aspects of the convexity hierarchy we refer to [10, 9, 15].

Arroyo et al. [10] showed that convex and h-convex drawings can be characterized via finitely many forbidden subconfigurations. A simple drawing is *convex* if and only if it does not contain $\Pi_{5,1}^{oc}$ or $\Pi_{5,2}^{oc}$ (cf. Figure 3) as a subconfiguration. Moreover, a convex drawing is *h-convex* if and only if it does not contain Π_6^{oh} (cf. Figure 4) as a subconfiguration.



■ **Figure 3** The two obstructions $\Pi_{5,1}^{oc}$ (left) and $\Pi_{5,2}^{oc}$ (right) for convex drawings. A triangle which is not convex is highlighted in red.



■ **Figure 4** The obstruction Π_6^{oh} for h-convex drawings. The convex side of the red triangle is the bounded side and for the blue triangle its the unbounded side.

Our framework by default enumerates rotation systems of simple drawings of K_n . To restrict the search space to convex drawings and h-convex drawings, one can use the flag `-c` and `-hc`, respectively. With these flags, $\Theta(n^5)$ (resp. $\Theta(n^6)$) clauses are added to forbid the configurations $\Pi_{5,1}^{oc}$ and $\Pi_{5,2}^{oc}$ (resp. Π_6^{oh}) as induced subconfigurations, similar as in Section 3.2.

4.2 C-Monotone and Strongly C-Monotone Drawings

A simple drawing \mathcal{D} in the plane is *c-monotone* if there is a point O such that every ray emanating from O intersects every edge of \mathcal{D} at most once. Moreover, \mathcal{D} is *strongly c-monotone* if, for every vertex v , there is a ray which does not intersect edges incident to v . More generally, we say that a rotation system is (strongly) c-monotone if it has a (strongly) c-monotone drawing. Even though on the first glance this definition seems to strongly depend on the actual drawing, Aichholzer et al. [5] proved the following combinatorial characterization: a rotation systems on elements $V = \{a_1, \dots, a_n\}$ is c-monotone if and only if it can be extended by two additional elements b_1, b_2 such that no two edges b_1a_i and b_2a_j cross. Moreover, it is strongly c-monotone if for every i there exists $j = j(i)$ such that the

star centered at a_i does not cross the edges $a_j b_1$ and $a_j b_2$. In our framework, the flags `-cm` and `-scm` restrict to c -monotone and strongly c -monotone rotations systems, respectively.

4.3 Generalized Twisted Drawings

A c -monotone drawing of K_n is *generalized twisted* if there is one ray emanating of the point O that intersects all edges of the drawing. This can be implemented in a similar way as above. As shown by Aichholzer et al. [4], generalized twisted drawings with $n \geq 7$ are exactly those simple drawings, where every subconfiguration on 5 elements is isomorphic to $\Pi_{5,1}^{oc}$. This combinatorial description can be encoded in terms of rotation systems by forbidding all other 4 possibilities for subconfigurations on 5 elements. This characterization can be activated in our framework using the flag `-gt`.

5 Applications and Showcases of our Framework

5.1 Plane Hamiltonian Substructures

One prominent conjecture on plane substructures in simple drawings of K_n is by Rafla.

► **Conjecture 5.1** (Rafla [41]). *Every simple drawing of K_n with $n \geq 3$ contains a plane Hamiltonian cycle.*

Rafla verified the conjecture for $n \leq 7$. Later Ábrego et al. [1] enumerated all rotation systems for $n \leq 9$ and verified Rafla’s conjecture. The conjecture was recently proven for the subclasses of cylindrical and strongly c -monotone drawings [8], for convex drawings [14], and for generalized twisted drawings with an odd number of vertices [5]. With our SAT framework, we got additional computational results.

► **Theorem 5.2.** *Conjecture 5.1 is true for all simple drawings with $n \leq 10$ and generalized twisted drawings with $n \leq 13$.*

We searched for a counterexample to the conjecture with the parameter `-HC`. For $n = 8, 9, 10$ the solver CaDiCaL took about 25 CPU seconds, 80 CPU minutes, and 3 CPU days, respectively, to show unsatisfiability. In the setting of generalized twisted drawings, the computations for $n = 12$ took about 3 CPU hours and the case $n = 13$ is covered in [5]. Furthermore, we exported a CNF file with parameter `-o` and ran the stand-alone executable of CaDiCaL to create a DRAT certificate. The certificate for $n = 10$ is about 78GB and the verification of the unsatisfiability took about 6 CPU days with the proof checking tool DRAT-trim [49]. The resources used for $n \leq 9$ are negligible.

Recently, Aichholzer et al. [8] provided a strengthening of Rafla’s conjecture:

► **Conjecture 5.3** ([8, Conjecture 1.2]). *For every simple drawing of K_n and for every choice of two vertices a, b , there is a plane Hamiltonian path from a to b .*

Similar to Rafla’s conjecture, this conjecture was verified using the database of rotation systems for $n \leq 9$. Moreover, it was proven for strongly c -monotone drawings, cylindrical, and convex drawings, see [8, 14]. To test Conjecture 5.3 with our framework, we use the flag `--forbidAllPairshP`. The computations for $n = 10$ took about 4 CPU days, and for the restricted setting of generalized twisted drawings about 5 CPU hours for $n = 13$.

► **Theorem 5.4.** *Conjecture 5.3 holds for $n \leq 10$ for simple drawings of K_n and for $n \leq 13$ for generalized twisted drawings.*

Another strengthening of Rafla’s conjecture was recently proposed by Bergold et al. [14]:

► **Conjecture 5.5** ([14, Conjecture 5.2]). *Every simple drawing of K_n contains a plane subdrawing with $2n - 3$ edges which contains a Hamiltonian cycle.*

As the main result of their article, they prove the conjecture for the subclass of convex drawings. We here use our SAT framework with parameter `-HC+` to verify the conjecture for simple drawings up to $n \leq 9$ vertices. The computations took about 3 CPU days.

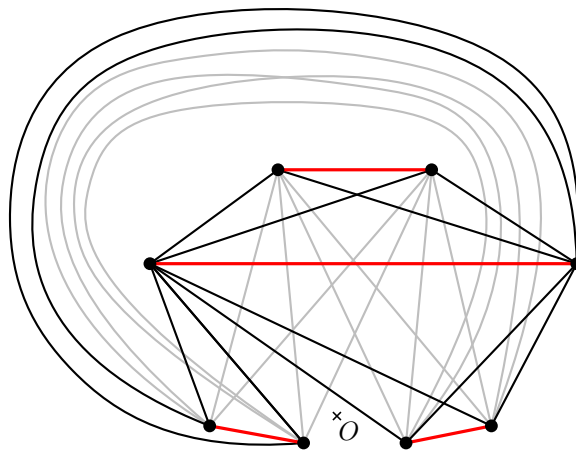
► **Theorem 5.6.** *Conjecture 5.5 holds for $n \leq 9$.*

While for the previous two conjectures, we continued the search for subclasses and larger n , the number of clauses in this encoding (cf. Appendix C.1) grew too fast to continue.

As shown in [14], there are several variants of prescribing structures for plane Hamiltonian subgraphs. However for simple drawings, we cannot even assign an edge to be contained in a Hamiltonian cycle. A weakening of this question is prescribing edges such that there is a Hamiltonian cycle which does not cross these edges (but not necessarily contain them). A natural question is to prescribe plane matchings and ask for a plane Hamiltonian cycle which together with the matching builds a plane Hamiltonian subgraph, i.e., the edges of the matching are not crossed by the Hamiltonian cycle (but possibly contained). For the setting of a geometric drawing of K_n Hoffmann and Tóth [34] showed that for every plane perfect matching M there exists a plane Hamiltonian cycle that does not cross any edge from M . See also [33] for a version with not necessarily perfect matchings.

While the statement does not generalize to the simple drawings and not even to strongly c-monotone (see Figure 5), our computations suggest that it is true for convex drawings. Hence, we dare another strengthening of Rafla’s conjecture:

► **Conjecture 5.7.** *For every plane matching M in a convex drawing of K_n there exists a plane Hamiltonian cycle that does not cross any edge from M .*



■ **Figure 5** A perfect matching (red) in a non-convex and strongly c-monotone drawing of K_8 , which does not contain a plane Hamiltonian cycle not crossing the matching edges. Edges which cross matching edges are marked in grey.

Using our framework and the parameter `-HT+ k`, where $k \in \{1, \dots, \lfloor n/2 \rfloor\}$ denotes the size of the matching, it took about 12 CPU days in total to verify the conjecture for $n \leq 11$. The details of the encoding are given in Appendix C.2.

► **Theorem 5.8.** *Conjecture 5.7 is true for $n \leq 11$.*

5.2 Empty k -Cycles

Another interesting strengthening of Rafla’s conjecture is formulated in terms of empty k -cycles. An *empty k -cycle* is a plane cycle through k vertices of the drawing such that all remaining vertices lie on one common side.

► **Conjecture 5.9** ([14, Conjecture 5.1]). *Every simple drawing of K_n contains an empty k -cycle for every $k = 3, \dots, n$.*

The case $k = n$ coincides with Rafla’s conjecture as empty k -cycles are precisely plane Hamiltonian cycles. Empty 3-cycles coincide with empty triangles and therefore the case $k = 3$ is shown by Harborth [26]. Bergold et al. [14] showed that the conjecture is true for the subclass of convex drawings. We used our SAT framework with parameter `--emptycycles k`, where k denotes the length of the empty cycle, to verify the conjecture for up to $n = 10$. Details of the encoding are deferred to Appendix C.3. Table 1 shows the computing times for different parameters of n and k . Note that the existence of empty n -cycles in all simple drawings of K_n imply the existence empty n -cycles in simple drawings of K_{n+1} . This is also reflected by computational data as the computing times for $k = n - 1$ are comparably small.

► **Theorem 5.10.** *Conjecture 5.9 holds for $n \leq 10$ for simple drawings.*

n/k	3	4	5	6	7	8	9	10
6	<0.1	<0.1	<0.1	<0.1				
7	0.2	1.0	0.6	0.1	1.1			
8	1.2	10.3	12.1	15.0	2.1	21.4		
9	3.7	46.0	337.0	1248.7	2732.7	30.1	1947.8	
10	17.3	467.5	5804.5	66600.3	414212.9	618399.9	2968.2	280384.4

■ **Table 1** Computing time for empty k -cycles in simple drawings of K_n in CPU seconds.

5.3 Uncrossed Edges

Next we focus on edges which are not crossed by any other edge. In 1964, Ringel [42] proved that in every simple drawing of K_n there are at most $2n - 2$ edges without a crossing. Later, Harborth and Mengersen [27] studied the minimal number of uncrossed edges. They showed that every simple drawing of K_n with $n \leq 7$ contains an uncrossed edge and constructed simple drawings for $n \geq 8$ such that every edge is crossed. The constructed drawings are strongly c -monotone but not convex. Moreover, they conjectured that crossing-maximal drawings, i.e., drawings with $\binom{n}{4}$ crossings, behave differently.

► **Conjecture 5.11** ([28]). *Every crossing-maximal simple drawing of K_n contains an uncrossed edge.*

We used the SAT framework with flags `-aec` (all edges crossed) and `-cmax` (crossing-maximal), we confirmed to verify Conjecture 5.11 for up to $n = 16$. The computations for $n = 14, 15, 16$ took about 3, 8, and 35 CPU hours, respectively.

► **Theorem 5.12.** *Conjecture 5.11 is true for $n \leq 16$*

When restricted to convex drawings, all drawings with $n \leq 10$ have an uncrossed edge. For $n = 11, \dots, 21$, there are h -convex drawings where every edge is crossed. The computations for $n = 22$ timed out after 8 CPU days. Kynčl and Valtr [38] showed that for sufficiently large n there is an h -convex drawing of K_n without uncrossed edge. We conjecture:

► **Conjecture 5.13.** *For $n \geq 11$ there is an h-convex drawing of K_n where every edge is crossed.*

5.4 Quasiplanarity and Crossing Families

In simple drawings there are not only unavoidable plane structures, but also unavoidable crossing structures. Given a drawing of K_n , a set of k independent edges that cross pairwise is called a k -crossing family. A simple drawing without a k -crossing family is called k -quasiplanar. Brandenburg [19] found a 3-quasiplanar drawing of K_{10} which is moreover h-convex and strongly c-monotone. As shown by Pitchanathan and Shannigrahi [40], no simple drawing of K_{11} is 3-quasiplanar, that is, every simple drawing of K_{11} contains a 3-crossing family. We reproduced this results with the SAT framework and parameter `-crf 3`, which forbids crossing families of size 3.

Aichholzer et al. [2] used complete enumeration to show that for $n \geq 9$ every geometric drawing of K_n has a 3-crossing family and this is the smallest possible value. Moreover, Aichholzer et al. [7] utilized SAT solvers to show that for $n \geq 15$ every geometric drawing of K_n has a 4-crossing family. Our framework found an h-convex drawing of K_{16} without a 4-crossing family after about 1 CPU day. We provide the example as supplemental data [16].

For crossing-maximal drawings there seem to be large crossing families:

► **Conjecture 5.14.** *Every crossing-maximal drawing of K_n contains a $\lfloor \frac{n}{2} \rfloor$ -crossing family.*

The computations for $n = 8, 10$ took about 2 CPU seconds and 2 CPU hours, respectively.

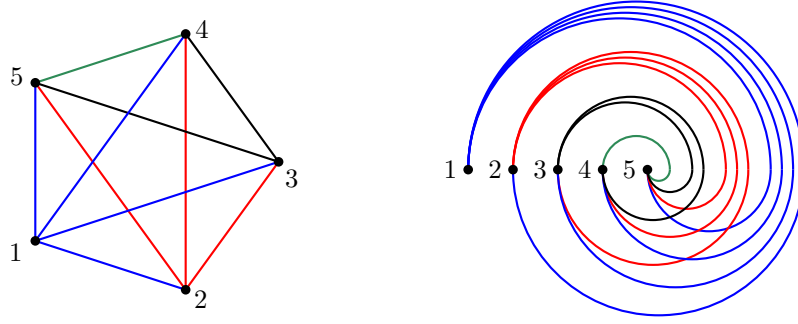
5.5 Generalized Erdős–Szekeres Theorem

The Erdős–Szekeres theorem asserts that every sufficiently large point set in the plane in general position contains a subset of k points in convex position (i.e., no point lies in the convex hull of the others). In the context of geometric drawings this immediately implies that every sufficiently large geometric drawing contains a subdrawing weakly isomorphic to the *perfect convex* drawing \mathcal{C}_k . Here \mathcal{C}_k denotes the geometric graph where the k vertices are in convex position. A drawing of K_k is weakly isomorphic to \mathcal{C}_k if and only if there exists a labeling $1, \dots, k$ of the vertices such that ac crosses bd for all $1 \leq a < b < c < d \leq k$. Recall that this defines the weak equivalence class of \mathcal{C}_k (Proposition A.2).

Harborth and Mengersen [28] showed that the Erdős–Szekeres theorem does not generalize to simple drawings. For every $k \geq 5$ the *perfect twisted* drawing \mathcal{T}_k does not contain a subdrawing weakly isomorphic to \mathcal{C}_5 . The perfect twisted drawing \mathcal{T}_k is characterized by the existence of a vertex labeling such that ad crosses bc if and only if $1 \leq a < b < c < d \leq k$. Figure 6 shows drawings of \mathcal{C}_5 and \mathcal{T}_5 .

Pach, Solymosi, and Tóth [39] proved an Erdős–Szekeres-type theorem for simple drawings: for all integers a and b there exists $N = N_s(\mathcal{C}_a, \mathcal{T}_b)$ such that for all $n \geq N$ every simple drawing of K_n contains \mathcal{C}_a or \mathcal{T}_b as a subdrawing. Suk and Zeng [48] showed the currently best bound: $N_s(\mathcal{C}_a, \mathcal{T}_b) \leq 2^{9(ab)^2 \log_2(a) \log_2(b)}$. For the class of c-monotone and strongly c-monotone we analogously define $N_{\text{cm}}(\mathcal{C}_a, \mathcal{T}_b)$ and $N_{\text{scm}}(\mathcal{C}_a, \mathcal{T}_b)$, respectively.

When restricting the question to convex drawings, the perfect twisted drawing \mathcal{T}_5 (cf. $\Pi_{5,1}^{\text{c}}$) does not occur. Hence every sufficiently large convex drawing contains a perfect convex \mathcal{C}_a . For the convex and h-convex drawings we can thus define the generalized Erdős–Szekeres numbers $N_{\text{cv}}(\mathcal{C}_a)$ and $N_{\text{hcv}}(\mathcal{C}_a)$, respectively, as the smallest integer n such that every convex (resp. h-convex) drawing of K_n contains \mathcal{C}_a as a subdrawing. The bound by Suk and Zeng [48] immediately gives $N_{\text{hcv}}(\mathcal{C}_a) \leq N_{\text{cv}}(\mathcal{C}_a) \leq 2^{O(a^2 \log a)}$. Similarly, when



■ **Figure 6** The two unavoidable configurations \mathcal{C}_5 (left) and \mathcal{T}_5 (right).

restricting to generalized twisted drawings, the perfect convex drawing \mathcal{C}_5 does not appear. Let $N_{\text{gt}}(\mathcal{T}_a)$ be the smallest integer n such that every generalized twisted drawing of K_n contains \mathcal{T}_a as a subdrawing. It holds $N_{\text{gt}}(\mathcal{T}_a) \leq 2^{O(a^2 \log a)}$ [48].

Using our SAT framework we determined the following values:

► **Theorem 5.15.** *It holds $N_s(\mathcal{C}_5, \mathcal{T}_5) = N_{\text{cm}}(\mathcal{C}_5, \mathcal{T}_5) = N_{\text{scm}}(\mathcal{C}_5, \mathcal{T}_5) = 13$, $N_{\text{cv}}(\mathcal{C}_5) = N_{\text{hcv}}(\mathcal{C}_5) = 11$, $N_{\text{gt}}(\mathcal{T}_6) = 7$, and $N_{\text{gt}}(\mathcal{T}_7) = 10$.*

The parameters `-C a` and `-T b` allow to forbid \mathcal{C}_a and \mathcal{T}_b , respectively. Furthermore we introduced the parameter `-X k` to forbid crossing-maximal subdrawings of K_k . Since \mathcal{C}_5 and \mathcal{T}_5 are the only two crossing-maximal drawings of K_5 , `-X 5` and `-C 5 -T 5` give equisatisfiable instances. It took about 8 CPU seconds to prove $N_{\text{cv}}(\mathcal{C}_5) \leq 11$ and 36 CPU hours to prove $N_s(\mathcal{C}_5, \mathcal{T}_5) \leq 13$. The tightness of the bounds is witnessed by examples showing $N_{\text{hcv}}(\mathcal{C}_5) > 10$ and $N_{\text{scm}}(\mathcal{C}_5, \mathcal{T}_5) > 12$. Moreover, the program found examples witnessing $N_{\text{hcv}}(\mathcal{C}_6) > 21$, $N_s(\mathcal{C}_6, \mathcal{T}_5) > 23$, $N_s(\mathcal{C}_5, \mathcal{T}_6) > 16$, and $N_{\text{gt}}(\mathcal{T}_8) > 12$; see the supplemental data [16].

The corresponding number for geometric drawings, $N_{\text{geom}}(\mathcal{C}_k)$, is the classical Erdős–Szekeres number. It is of order $2^{k+o(k)}$ [47]. This motivates the question, whether one of the above Ramsey numbers, in particular $N_{\text{scm}}(\mathcal{C}_a, \mathcal{T}_a)$, $N_{\text{gt}}(\mathcal{T}_a)$, and $N_{\text{hcv}}(\mathcal{C}_a)$, can also be bounded by an exponential function c^a for some constant c .

5.6 Number of Empty Triangles

An *empty triangle* in a simple drawing of K_n is a triangle induced by three vertices such that the interior of one of its two sides does not contain any vertex. Let $\Delta(n)$ denote the minimum number of empty triangles in all simple drawings of K_n . Harborth [26] proved the bounds $2 \leq \Delta(n) \leq 2n - 4$ and conjectured the upper bound to be optimal.

► **Conjecture 5.16** ([26]). *It holds $\Delta(n) = 2n - 4$.*

In a recent paper, García et al. [24] showed that generalized twisted drawings have exactly $2n - 4$ empty triangles. Ruiz–Vargas [43] proved $\Delta(n) \geq \frac{2n}{3}$. The bound was further improved by Aichholzer et al. [6] to $\Delta(n) \geq n$. Moreover, Ábrego et al. [6, 1] used the database of rotation systems to show that $\Delta(n) = 2n - 4$ holds for $n \leq 9$. We reproduced this result and further verified the conjecture for $n = 10$ with our SAT framework. The parameter `-etupp k` asserts that there are at most k empty triangles; see Appendix C.4 for more details on the encoding. The computations for $n = 7, 8, 9, 10$ took about 10 CPU seconds, 25 CPU minutes, 46 CPU hours, and 16 CPU days respectively.

► **Theorem 5.17.** *Conjecture 5.16 is true for $n \leq 10$.*

Moreover, it is known that every convex drawing of K_n contains at least $\Delta_{cv}(n) \geq \Omega(n^2)$ empty triangles [9], which is asymptotically tight as there exist geometric drawings with $\Theta(n^2)$ empty triangles [13]. Determining the minimum number of empty triangles in geometric drawings $\Delta_{geom}(n)$ remains a challenging problem cf. [20, Chapter 8.4] and [3].

5.7 Enumeration

Last but not least, our framework can be used with the parameter `-a` to enumerate the solutions of a CNF. This in particular allows to count isomorphism classes of various classes of drawings; see Table 2. It is also possible to enumerate examples from the intersection of various classes by simply activating the desired flags, e.g., `-hc -scm` restricts to rotation systems that are both h-convex and strongly c-monotone. However, for enumeration and counting, classic approaches such as the Avis–Fukuda reverse search technique [11] (as used in [1]) seem to be better suited. For SAT solvers that are based on the CDCL algorithm, one needs to add a clause for every found solution to prevent it from reappearing and therefore the size of the instance and the memory consumption grows linear in the number of objects.

	all	convex	h-convex	c-monotone	str. c-monotone	gen. twisted
n = 4	2	2	2	2	2	1
n = 5	5	3	3	5	5	1
n = 6	102	16	15	102	95	3
n = 7	11 556	139	126	11 556	8 373	9
n = 8	5 370 725*	3 853	3 394	?	?	32
n = 9	7 198 391 729*	215 105	183 982	?	?	115

■ **Table 2** Number of isomorphism classes of simple drawings of K_n . The entries marked with * were computed in [1] and were not verified by our framework.

6 Discussion

To tackle a comprehensive list of conjectures on simple drawings of K_n , we developed SAT encodings for various properties and subclasses. Our highly parameterized python framework allows to create a CNF instance such that the solutions correspond to drawings with specified properties. Modern SAT solvers are used to decide whether there exist such drawings.

To optimize the overall performance, we experimented with the optimization tool SBVA [25]. It introduces auxiliary variables into a CNF to reduce the number of clauses while preserving equisatisfiability. Even though this approach does not always lead to a better performance of the SAT solver, we analyzed all instances where SBVA lead to a speedup and incorporated the learned patterns into our encoding.

Note that every CNF can be partitioned into independent parts (so-called cubes) which can then be solved in parallel [31]. However, it is a highly non-trivial task to find a good partition such that all cubes are of similar complexity and a bad partitioning can lead to significantly worse computing times in total.

Aesthetic drawings

Given the abstract graph of a planarization corresponding to drawing D of a rotation system, we can find a plane drawing with explicit coordinates from the $m \times m$ integer grid by applying

Schnyder’s algorithm [46], where m denotes the number of vertices of the planarization. Such drawings on the grid however do not look very aesthetic because vertices can be very close to edges and faces may be represented by arbitrary polygons. Instead we compute the embedding using iterated Tutte embeddings to create an aesthetic visualization of the planarization, where every face is drawn convex and edges and faces are within a certain ratio. We used a slight modification of the implementation from Felsner and Scheucher [22], see also the `visualize.sage` script in [44]. Based on this drawing of the planarization, we visualize the original drawing of K_n by drawing its edges as a Beziér curve, as illustrated in the computer-generated graphic Figure 9 in the appendix. Note that each original edge consists of a sequence of edges in the planarization.

References

- 1 Bernardo M. Ábrego, Oswin Aichholzer, Silvia Fernández-Merchant, Thomas Hackl, Jürgen Pammer, Alexander Pilz, Pedro Ramos, Gelasio Salazar, and Birgit Vogtenhuber. All good drawings of small complete graphs. In *Proceedings of the 31st European Workshop on Computational Geometry (EuroCG 2015)*, pages 57–60, 2015. URL: <http://eurocg15.fri.uni-lj.si/pub/eurocg15-book-of-abstracts.pdf>.
- 2 Oswin Aichholzer, Franz Aurenhammer, and Hannes Krasser. Enumerating Order Types for Small Point Sets with Applications. *Order*, 19(3):265–281, 2002. doi:10.1023/A:1021231927255.
- 3 Oswin Aichholzer, Martin Balko, Thomas Hackl, Jan Kynčl, Irene Parada, Manfred Scheucher, Pavel Valtr, and Birgit Vogtenhuber. A superlinear lower bound on the number of 5-holes. *Journal of Combinatorial Theory, Series A*, 173:105236, 2020. doi:10.1016/j.jcta.2020.105236.
- 4 Oswin Aichholzer, Alfredo García, Javier Tejel, Birgit Vogtenhuber, and Alexandra Weinberger. Characterizing rotation systems of generalized twisted drawings via 5-tuples. In *Proceedings of the 20th Spanish Meeting on Computational Geometry (EGC 2023)*, page 71, 2023. URL: https://egc23.web.uah.es/wp-content/uploads/2023/06/EGC23_paper_18.pdf.
- 5 Oswin Aichholzer, Alfredo García, Javier Tejel, Birgit Vogtenhuber, and Alexandra Weinberger. Twisted ways to find plane structures in simple drawings of complete graphs. *Discret. Comput. Geom.*, 71(1):40–66, 2024. doi:10.1007/S00454-023-00610-0.
- 6 Oswin Aichholzer, Thomas Hackl, Alexander Pilz, Pedro Ramos, Vera Sacristán, and Birgit Vogtenhuber. Empty triangles in good drawings of the complete graph. *Graphs and Combinatorics*, 31:335–345, 2015. doi:10.1007/s00373-015-1550-5.
- 7 Oswin Aichholzer, Jan Kynčl, Manfred Scheucher, Birgit Vogtenhuber, and Pavel Valtr. On crossing-families in planar point sets. *Computational Geometry*, 107:101899, 2022. doi:10.1016/j.comgeo.2022.101899.
- 8 Oswin Aichholzer, Joachim Orthaber, and Birgit Vogtenhuber. Towards crossing-free Hamiltonian cycles in simple drawings of complete graphs. *Computing in Geometry and Topology*, 3(2):5:1–5:30, 2024. doi:10.57717/cgt.v3i2.47.
- 9 Alan Arroyo, Dan McQuillan, R. Bruce Richter, and Gelasio Salazar. Levi’s Lemma, pseudo-linear drawings of K_n , and empty triangles. *Journal of Graph Theory*, 87(4):443–459, 2018. doi:10.1002/jgt.22167.
- 10 Alan Arroyo, Dan McQuillan, R. Bruce Richter, and Gelasio Salazar. Convex drawings of the complete graph: topology meets geometry. *Ars Mathematica Contemporanea*, 22(3), 2022. doi:10.26493/1855-3974.2134.ac9.
- 11 David Avis and Komei Fukuda. Reverse search for enumeration. *Discrete Applied Mathematics*, 65(1):21–46, 1996. First International Colloquium on Graphs and Optimization. doi:10.1016/0166-218X(95)00026-N.
- 12 Martin Balko and Pavel Valtr. A SAT attack on the Erdős–Szekeres conjecture. *European Journal of Combinatorics*, 66:13–23, 2017. doi:10.1016/j.ejc.2017.06.010.

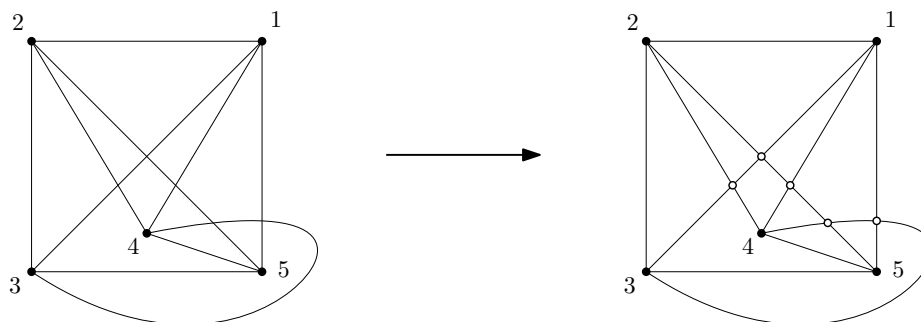
- 13 Imre Bárány and Zoltán Füredi. Empty simplices in Euclidean space. *Canadian Mathematical Bulletin*, 30(4):436–445, 1987. doi:10.4153/cmb-1987-064-1.
- 14 Helena Bergold, Stefan Felsner, Meghana M. Reddy, Joachim Orthaber, and Manfred Scheucher. Plane Hamiltonian Cycles in Convex Drawings. In *40th International Symposium on Computational Geometry (SoCG 2024)*, volume 293 of *LIPIcs*, pages 18:1–18:16, 2024. doi:10.4230/LIPIcs.SocG.2024.18.
- 15 Helena Bergold, Stefan Felsner, Manfred Scheucher, Felix Schröder, and Raphael Steiner. Topological Drawings meet Classical Theorems from Convex Geometry. In *Discrete & Computational Geometry*, 70:1121–1143, 2023. doi:10.1007/s00454-022-00408-6.
- 16 Helena Bergold and Manfred Scheucher. Supplemental source code and data. <https://github.com/manfredscheucher/rotsys-sat>.
- 17 Armin Biere. CaDiCaL at the SAT Race 2019. In *Proc. of SAT Race 2019 – Solver and Benchmark Descriptions*, volume B-2019-1 of *Department of Computer Science Series*, pages 8–9. University of Helsinki, 2019. URL: <http://researchportal.helsinki.fi/en/publications/proceedings-of-sat-race-2019-solver-and-benchmark-descriptions>.
- 18 Armin Biere, Marijn Heule, Hans van Maaren, and Toby Walsh, editors. *Handbook of Satisfiability*, volume 336 of *Frontiers in Artificial Intelligence and Applications*. IOS Press, 2021.
- 19 Franz J. Brandenburg. A simple quasi-planar drawing of K_{10} . In *Proceedings of the 24th International Symposium on Graph Drawing and Network Visualization*, volume 9801 of *LNCS*, pages 603–604. Springer, 2016. doi:10.1007/978-3-319-50106-2.
- 20 Peter Brass, William O. J. Moser, and János Pach. *Research Problems in Discrete Geometry*. Springer, 2005. doi:10.1007/0-387-29929-7.
- 21 Curtis Bright, Kevin K. H. Cheung, Brett Stevens, Ilias S. Kotsireas, and Vijay Ganesh. A SAT-based Resolution of Lam’s Problem. In *35th Conference on Artificial Intelligence (AAAI-21)*, pages 3669–3676, 2021. doi:10/kxrx.
- 22 Stefan Felsner and Manfred Scheucher. Arrangements of Pseudocircles: Triangles and Drawings. *Discrete & Computational Geometry*, 65:261–278, 2021. doi:10.1007/s00454-020-00173-4.
- 23 Stefan Felsner and William T. Trotter. Posets and planar graphs. *Journal of Graph Theory*, 49(4):273–284, 2005. doi:10.1002/jgt.20081.
- 24 Alfredo García, Javier Tejel, Birgit Vogtenhuber, and Alexandra Weinberger. Empty triangles in generalized twisted drawings of K_n . In *Proceedings of the 30th International Symposium on Graph Drawing and Network Visualization (GD 2022)*, volume 13764 of *LNCS*, pages 40–48. Springer, 2022. doi:10.1007/978-3-031-22203-0_4.
- 25 Andrew Haberlandt, Harrison Green, and Marijn J. H. Heule. Effective Auxiliary Variables via Structured Reencoding. In *26th International Conference on Theory and Applications of Satisfiability Testing (SAT 2023)*, volume 271 of *Leibniz International Proceedings in Informatics (LIPIcs)*, pages 11:1–11:19. Schloss Dagstuhl – Leibniz-Zentrum für Informatik, 2023. doi:10.4230/LIPIcs.SAT.2023.11.
- 26 Heiko Harborth. Empty triangles in drawings of the complete graph. *Discrete Mathematics*, 191(1-3):109–111, 1998. doi:10.1016/S0012-365X(98)00098-3.
- 27 Heiko Harborth and Ingrid Mengersen. Edges without crossings in drawings of complete graphs. *Journal of Combinatorial Theory, Series B*, 17(3):299–311, 1974.
- 28 Heiko Harborth and Ingrid Mengersen. Drawings of the complete graph with maximum number of crossings. *Congressus Numerantium*, pages 225–225, 1992.
- 29 Marijn J. H. Heule. Schur number five. In *32nd Conference on Artificial Intelligence (AAAI-18)*, pages 6598–6606, 2018. doi:10/kxrt.
- 30 Marijn J. H. Heule, Oliver Kullmann, and Victor W. Marek. Solving and Verifying the Boolean Pythagorean Triples Problem via Cube-and-Conquer. In *19th International Conference on Theory and Applications of Satisfiability Testing (SAT 2016)*, pages 228–245. Springer, 2016. doi:10/gkkscn.

- 31 Marijn J. H. Heule, Oliver Kullmann, Siert Wieringa, and Armin Biere. Cube and Conquer: Guiding CDCL SAT Solvers by Lookaheads. In *Hardware and Software: Verification and Testing*, pages 50–65. Springer, 2012. doi:10/f3ss29.
- 32 Marijn J. H. Heule and Manfred Scheucher. Happy ending: An empty hexagon in every set of 30 points. In Bernd Finkbeiner and Laura Kovács, editors, *Proc. 30th International Conference on Tools and Algorithms for the Construction and Analysis of Systems (TACAS'24)*, volume 14570 of *LNCS*, pages 61–80. Springer, 2024. doi:10.1007/978-3-031-57246-3_5.
- 33 Michael Hoffmann. *On the existence of paths and cycles*. Doctoral thesis, ETH Zurich, Zürich, 2005. doi:10.3929/ethz-a-004945082.
- 34 Michael Hoffmann and Csaba D. Tóth. Segment endpoint visibility graphs are Hamiltonian. *Computational Geometry*, 26(1):47–68, 2003. doi:10.1016/S0925-7721(02)00172-4.
- 35 Markus Kirchweber, Manfred Scheucher, and Stefan Szeider. SAT-based generation of planar graphs. In *26th International Conference on Theory and Applications of Satisfiability Testing (SAT 2023)*, volume 271 of *LIPICs*, pages 14:1–14:17. Dagstuhl, 2023. doi:10.4230/LIPICs.SAT.2023.14.
- 36 Jan Kynčl. Enumeration of simple complete topological graphs. *European Journal of Combinatorics*, 30(7):1676–1685, 2009. doi:10.1016/j.ejc.2009.03.005.
- 37 Jan Kynčl. Simple realizability of complete abstract topological graphs simplified. *Discrete & Computational Geometry*, 64:1–27, 2020. doi:10.1007/s00454-020-00204-0.
- 38 Jan Kynčl and Pavel Valtr. On edges crossing few other edges in simple topological complete graphs. *Discrete Mathematics*, 309(7):1917–1923, 2009. doi:10.1016/j.disc.2008.03.005.
- 39 János Pach, József Solymosi, and Géza Tóth. Unavoidable configurations in complete topological graphs. *Discrete & Computational Geometry*, 30(2):311–320, 2003. doi:10.1007/s00454-003-0012-9.
- 40 Arjun Pitchanathan and Saswata Shannigrahi. On the simple quasi crossing number of K_{11} . In *Proc. of Graph Drawing and Network Visualization*, volume 11904 of *LNCS*, pages 612–614. Springer, 2019. doi:10.1007/978-3-030-35802-0.
- 41 Nabil H. Raffle. *The good drawings D_n of the complete graph K_n* . PhD thesis, McGill University, Montreal, 1988. URL: <http://escholarship.mcgill.ca/concern/theses/x346d4920>.
- 42 Gerhard Ringel. Extremal problems in the theory of graphs. In *Theory of Graphs and its Applications (Proc. Sympos. Smolenice, 1963)*, volume 8590. Publ. House Czechoslovak Acad. Sci Prague, 1964.
- 43 Andres J. Ruiz-Vargas. Empty triangles in complete topological graphs. *Electronic Notes in Discrete Mathematics*, 44:169–174, 2013. doi:10.1016/j.endm.2013.10.026.
- 44 Manfred Scheucher. Supplemental source code for pseudocircle arrangements. <https://github.com/manfredscheucher/pseudocircle-arrangements-tools>.
- 45 Walter Schnyder. Planar graphs and poset dimension. *Order*, 5:323–343, 1989. doi:10.1007/BF00353652.
- 46 Walter Schnyder. Embedding planar graphs on the grid. In *Proceedings of the First Annual ACM-SIAM Symposium on Discrete Algorithms (SODA 1990)*, pages 138–148. Society for Industrial and Applied Mathematics, 1990.
- 47 Andrew Suk. On the Erdős–Szekeres convex polygon problem. *Journal of the American Mathematical Society*, 30:1047–1053, 2017. doi:10.1090/jams/869.
- 48 Andrew Suk and Ji Zeng. Unavoidable patterns in complete simple topological graphs. In *Proceedings of the 30th International Symposium on Graph Drawing and Network Visualization (GD 2022)*, volume 13764 of *LNCS*, pages 3–15. Springer, 2022. doi:10.1007/978-3-031-22203-0_1.
- 49 Nathan Wetzler, Marijn J. H. Heule, and Warren A. Hunt. DRAT-trim: Efficient Checking and Trimming Using Expressive Clausal Proofs. In *Theory and Applications of Satisfiability Testing (SAT 2014)*, volume 8561 of *LNCS*, pages 422–429. Springer, 2014. doi:10.1007/978-3-319-09284-3.

A SAT Encoding for Drawability of Pre-Rotation Systems

To give an independent proof of Proposition 2.2, we model a CNF for deciding whether a given pre-rotation system is drawable.

In the following, we set up the desired Boolean formula that encodes a potential planarization – if one exists. The *planarization* of a given drawing \mathcal{D} is the planar graph G obtained by placing an auxiliary *cross-vertex* at the position of every crossing point of \mathcal{D} and accordingly subdividing the two crossing edges. Each cross-vertex has degree four and increases the number of edges by two. Figure 7 gives an illustration.



■ **Figure 7** (left) A simple drawing of K_5 and (right) its planarization. The auxiliary cross-vertices are depicted as circles.

To decide whether a given pre-rotation system Π is drawable we need to find a planarization of a drawing belonging to Π . By Lemma 2.1(i) Π is not drawable if it contains Π_4^o . Hence we assume that Π is Π_4^o -free. Now Lemma 2.1(ii) implies that the pairs of crossing edges X can be inferred from the induced 4-tuples. In particular, for each edge $e \in E$ we know which crossings X_e occur along it. The missing information to get a planarization – if there exists one – is the order of the crossings along the edges.

For every edge $e = \{u, v\} \in E$ with $u < v$, let Σ_e be a permutation of the crossings X_e along e , which we extend by adding u as the first element and v as the last element. We define the graph G_Σ where the vertex set consists of the original elements $[n]$ and the crossings X , and for every $e = \{u, v\} \in E$ with $u < v$, we connect every pair of consecutive crossings from Σ_e .

Our aim is to find an assignment for all permutations Σ_e , $e \in E$, such that the corresponding graph G_Σ is a planar graph. To ensure that the desired graph is planar, we use Schnyder’s characterization of planar graphs [45], which we describe in more detail in Appendix B.

► **Proposition A.1.** *Let Π be a pre-rotation system. If Π is drawable, then there exists an assignment Σ such that G_Σ is planar. Moreover, every planar G_Σ is the planarization of a drawing with rotation system Π .*

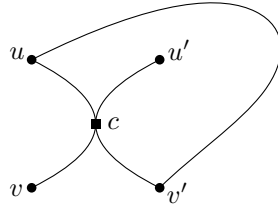
Proof. The first part is straight-forward. If Π is drawable, we consider a drawing and obtain G_Σ as its planarization.

For the second part, suppose that G_Σ is a planar graph and consider a plane drawing \mathcal{D} of G_Σ . We show that

- (i) the auxiliary cross-vertices are drawn as proper crossings; and
- (ii) the rotation system $\Pi_{\mathcal{D}}$ of the drawing \mathcal{D} equals Π .

To show (i), suppose that the cross-vertex c of the edges $\{u, v\}$ and $\{u', v'\}$ of K_n is drawn as a touching, i.e., the endpoints of the edges are consecutive in the cyclic order around c . Without loss of generality we assume that they appear as follows u, v, v', u' . We consider the planarization of the subdrawing of K_n induced by the four vertices u', v', v, u . Since a K_4 has at most one crossing, c is the only crossing vertex in this subdrawing. As illustrated in Figure 8 not all edges of this planarization of K_4 can be drawn without crossings, which is a contradiction. Hence, in \mathcal{D} all crossing-vertices are drawn as proper crossings.

Since the pairs of crossing edges are the same for Π and $\Pi_{\mathcal{D}}$, (ii) follows from the following Proposition A.2. ◀



■ **Figure 8** The vertices u' and v cannot be connected in a plane way.

► **Proposition A.2.** *Let Π and Π' be two Π_4^0 -free pre-rotation systems on $[n]$. The pairs of crossing edges of Π and Π' coincide if and only if Π is equal to Π' or its reflection.*

A weaker version of Proposition A.2 (restricted to rotation systems) was already proven by Kynčl [37, Proposition 2.1(1)].

Proof. If Π is equal to Π' or its reflection, then the pairs of crossing edges clearly coincide (Lemma 2.1(ii)).

For the converse statement, assume that Π differs from Π' and its reflection. We show that we find a set of five vertices $I \subset V$ such that, when restricted to I , the (sub-)pre-rotation system $\Pi|_I$ still differs from $\Pi'|_I$ and its reflection.

Case 1: there exists a vertex v such that the cyclic permutation π_v differs from π'_v and its reflection. Then there are four elements $J = \{a, b, c, d\}$ such that, when restricted to J , the cyclic permutation $\pi_v|_J$ still differs from $\pi'_v|_J$ and its reflection. Hence we can choose $I = \{v, a, b, c, d\}$.

Case 2: for every vertex v the cyclic permutation π_v is equal to π'_v or its reflection. Since Π differs from Π' and its reflection, there are two vertices v, w such that π_v equals π'_v and π_w equals the reflection of π'_w . By choosing any a, b, c distinct from v and w , we have five vertices $I = \{v, w, a, b, c\}$ such that a, b, c occur in the same order around v and a, b, c occur in the opposite order around w .

Using the program we enumerated all Π_4^0 -free pre-rotation systems on 5 vertices. This can be done with the command

```
python rotsys.py 5 -v5 -a --nat --checkATgraphs
```

As checked by the flag `--checkATgraphs`, any such two pre-rotation systems which are not reflections of each other have distinct pairs of crossing edges. Hence the pairs of crossing edges for Π and Π' are different. ◀

► **Proposition 2.2** ([1]). *A pre-rotation system on $n \leq 6$ elements is drawable if and only if it does not contain Π_4^0 , $\Pi_{5,1}^0$, or $\Pi_{5,2}^0$ (cf. Figure 2) as a subconfiguration.*

Proof. We combine the SAT frameworks from Section 3 for pre-rotation systems and from Appendix B for planar graphs. As a first step, we use the SAT framework to enumerate the 3 non-isomorphic pre-rotation systems on 4 elements using the command

```
python rotsys.py 4 -v4 -a -1
```

By Lemma 2.1(i) we know that there are exactly two non-isomorphic rotation systems on 4 vertices and the non-drawable pre-rotation system Π_4^o . Next, we enumerate the 7 non-isomorphic pre-rotation systems on 5 vertices, that do not contain Π_4^o .

```
python rotsys.py 5 -v5 -a -1 -r2f all5.json0
```

Our drawability framework shows that exactly five of them are drawable.

```
sage rotsys_draw.sage all5.json0
```

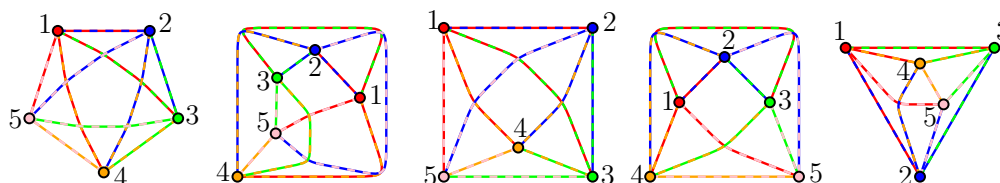
See Figure 9 for the computer generated¹ drawings of K_5 . The two configurations $\Pi_{5,1}^o$ and $\Pi_{5,2}^o$ are not drawable. Last but not least, we use the framework with the command

```
python rotsys.py 6 -a -1 -r2f all6.json0
```

to enumerate 102 non-isomorphic Π_4^o , $\Pi_{5,1}^o$, $\Pi_{5,2}^o$ - free pre-rotation systems on 6 elements. With the drawing framework we verify that all of them are drawable.

```
sage rotsys_draw.sage all6.json0
```

This completes the proof of Proposition 2.2. ◀



■ **Figure 9** Computer generated drawings of the five types of rotation systems on 5 elements.

B SAT encoding for planar graphs

Schnyder [45] characterized planar graphs as graphs whose incidence poset is of order dimension at most three. That is, a graph $G = (V, E)$ is planar if and only if there exist three total orders $\prec_1, \prec_2, \prec_3$ such that for every edge $\{u, v\} \in E$ and every vertex $w \in V \setminus \{u, v\}$ it holds $u \prec_i w$ and $v \prec_i w$ for some $i \in \{1, 2, 3\}$. This characterization allows to encode planarity in terms of a Boolean formula. Besides the fact that this approach can be used for planarity testing, it can also be used to enumerate all planar graphs with a specified property or to decide that no planar graphs with this property exists. It is worth noting that certain subclasses of planar graphs such as outer-planar graphs can be characterized in a similar fashion; see [23]. For further literature and other planarity encodings suitable for SAT-based investigations we refer the interested reader to Kirchweger et al. [35].

¹ We used iterated Tutte embeddings [22] to automatically generate aesthetic visualizations of the planarizations. Edges are drawn as a Beziér curve to make the visualization even more appealing.

For every pair of vertices $u, v \in V$ with $u \neq v$ we use Boolean variables $A_{u,v}$ to encode whether $\{u, v\}$ is an edge in the graph and, for any $i \in \{1, 2, 3\}$, we use Boolean variables $B_{i,u,v}$ to encode whether $u \prec_i v$. To assert that the Y variables indeed model a total order, we must ensure the linear order and anti-symmetry with the constraints $B_{i,u,v} \vee B_{i,v,u}$ and $\neg B_{i,u,v} \vee \neg B_{i,v,u}$ and transitivity with the constraints $\neg B_{i,u,v} \vee \neg B_{i,v,w} \vee B_{i,u,w}$ for every $i \in \{1, 2, 3\}$ and distinct $u, v, w \in V$.

To ensure Schnyder's planarity conditions, we introduce auxiliary variables $B_{i,u,v,w}$ to encode whether $u \prec_i w$ and $v \prec_i w$ holds for any three distinct variables u, v, w and $i \in \{1, 2, 3\}$ (that is, $B_{i,u,v,w} = B_{i,u,w} \vee B_{i,v,w}$) and then assert $\neg A_{u,v} \vee \bigvee_{i=1}^3 B_{i,u,v,w}$.

C Detailed Encodings

C.1 Plane Substructures

To assert that a subset of the edges $E' \subset E(K_n)$ does forms a plane subdrawing, we set the corresponding crossing variables to **False**, that is, we have a unit-clause $\neg C_{e,f}$ for every pair of non-adjacent edges $e, f \in E'$. Similarly, we can assert that E' does not form a plane subdrawing with the clause $\bigvee_{e,f \in E': e \cap f = \emptyset} C_{e,f}$.

To assert that there is no plane Hamiltonian cycle, we assert that for every permutation π there is at least one crossing pair in the set of edges $E_\pi = \{(\pi(i), \pi(i+1)) : i \in [n]\}$, where $\pi(n+1) = \pi(1)$. The encoding comes with $(n-1)!$ clauses and is only suited for small values of n . Similarly, we can deal with plane Hamiltonian subdrawings on $2n-3$ edges: We assert that there is at least one crossing formed by every edge set $E' \in \binom{E(K_n)}{2n-3}$ which contains the edges E_π of some Hamiltonian cycle π .

C.2 Extending Plane Matchings

To be more specific about the encoding for testing Conjecture 5.7, that is, searching plane Hamiltonian cycles for a prescribed matching: we assume towards a contradiction that there exists a convex drawing of K_n which has a plane matching $M = \{\{1, 2\}, \dots, \{2k-1, 2k\}\}$ with $2k \leq n$ such that every plane Hamiltonian cycle C crosses at least one edge of M . Note that M and C may share edges. As we fix the vertices of M , we cannot further assume without loss of generality that the rotation system is natural for $k \geq 2$. However, to speed up the computations, we break further symmetries in the search space:

- for every edge $\{u, u+1\} \in M$: $X_{1,2,u,u+1} = \text{True}$, that is, 1 sees 2, $u, u+1$ in this order;
- for every two edges $\{u, u+1\}, \{u', u'+1\} \in M$ with $u < u'$: $X_{1,2,u,u'} = \text{True}$, that is, 1 sees 2, u, u' in this order;
- for every $x, y \in [n] \setminus \{1, \dots, 2k\}$ with $x < y$: $X_{1,2,x,y} = \text{True}$, that is, 1 sees 2, x, y in this order.

C.3 Empty k -Cycles

Next we outline our encoding for empty k -cycles. The vertices π_1, \dots, π_k form an empty k -cycles if and only if it forms a plane k -cycle and all other vertices lie on one common side of the cycle. Let $E_\pi = \{(\pi_i, \pi_{i+1}) : i = 1, \dots, k\}$ with $\pi_{k+1} = \pi_1$ be the edges of the cycle. The first part can easily be formulated as using our auxiliary crossing variables. For the second part we need to introduce auxiliary variables $W_{\pi,p,q}$ that indicate whether the edge pq intersects an odd number of edges from E_π . Since we only consider simple drawings, the W variable indicates whether p and q lie in distinct sides. To assign the $W_{\pi,p,q}$ variable, we

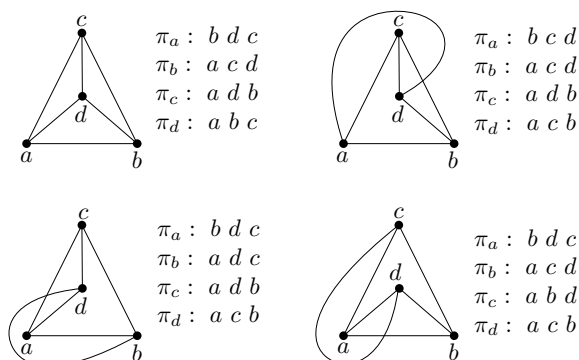
consider each of the 2^k cases how pq may intersect E_π and assign True or False, depending on whether the number of crossings with E_π even or odd. Note that this gives $n^k 2^k$ clauses in total. Ultimately, we forbid that π_1, \dots, π_k forms an empty k -cycles using the clauses

$$\bigvee_{e,f \in E_\pi} C_{e,f} \vee \bigvee_{p,q} W_{\pi,p,q}.$$

C.4 Empty Triangles

Empty triangles are exactly the empty 3-cycles and hence the encoding from Appendix C.3 can be used. However, since it comes with n^5 auxiliary variables, we now describe a more compact encoding that suffices with only n^3 auxiliary variables.

We distinguish the two sides of a triangle. For a triangle spanned by three distinct vertices a, b, c , one of its sides sees a, b, c in clockwise order and the other one in counterclockwise order. We denote by $S_{a,b,c}$ the side of the triangle which has a, b, c in counterclockwise order. In each of the drawings in Figure 10, $S_{a,b,c}$ is the bounded side and $S_{a,c,b}$ is the unbounded side. For every three distinct indices a, b, c we introduce a Boolean variable $E_{a,b,c}$ which is True if the side $S_{a,b,c}$ is empty. To assert the E variables, we introduce auxiliary variables. For a point $d \in [n] \setminus \{a, b, c\}$, we define $E_{a,b,c}^d = \text{False}$ if $S_{a,b,c}$ contains d . For four elements, there exist eight rotation systems, the four rotation systems in Figure 1 and their reflections. Hence, we set the variable $E_{a,b,c}^d$ to False if and only if one of the four cases depicted in Figure 10 occurs.



■ **Figure 10** The four cases where $S_{a,b,c}$ contains d .

The side $S_{a,b,c}$ is empty if and only if no point d lies in $S_{a,b,c}$, hence

$$E_{a,b,c} = \bigwedge_{d \in [n] \setminus \{a,b,c\}} E_{a,b,c}^d.$$